Tidally Induced Eddies Dominate Dispersal of the Thermal Plume from the Third Nuclear Power Plant in the Semi-enclosed Nan Wan Bay

Hung-Jen Lee *, Shih-Jen Huang, Pei-Jie Meng, Chung-Chi Chen, Chia-Ying Ho, Yi-Chen Tsai

Posted Date: 3 January 2024

doi: 10.20944/preprints202401.0098.v1

Keywords: shipboard ADCP; seasonal monsoon; MITgcm; tidal currents; thermal plume

Article

Tidally Induced Eddies Dominate Dispersal of the Thermal Plume from the Third Nuclear Power Plant in the Semi-Enclosed Nan Wan Bay

Hung-Jen Lee [1,*], Shih-Jen Huang [1], Pei-Jie Meng [2], Chung-Chi Chen [3], Chia-Ying Ho [1] and Yi-Chen Tsai [1]

[1] Department of Marine Environmental Informatics, National Taiwan Ocean University, Keelung 202301, Taiwan; lecgyver@mail.ntou.edu.tw(H.-J.L.); huangsj@mail.ntou.edu.tw(S.-J.H.); 20781001@mail.ntou.edu.tw(C.-Y.H.); eason10837@gmail.com(Y.-C.T.)
[2] Institute of Marine Biology, National Dong Hwa University, No. 2 Houwan Road, Checheng,Pingtung 94450, Taiwan; pjmeng@gms.ndhu.edu.tw(P.-J.M.)
[3] Department of Life Science, National Taiwan Normal University, Taipei 11677, Taiwan; ccchen@ntnu.edu.tw(C.- C.C.)
* Correspondence: Correspondence: lecgyver@mail.ntou.edu.tw

Abstract: In order to assess the range of impact of thermal wastewater discharge from the third Nuclear Power Plant (NP_No.3) on the local ecosystem, a three-dimensional ocean model (MITgcm) driven by tidal and climatological forcings is employed to study the present work. Tides and daily wind forcings are incorporated into the MITgcm model to examine their effects on the thermal plume and the water circulation in Nan Wan Bay. The model results reveal that the thermal plume is most likely to disperse to the southwest in summer; it is unlikely to drift to the southeast or northeast because of the presence of gentle southwesterly monsoon. In winter, the thermal plume is most likely to be directed to the southwest but barely visible in the northeast or southeast directions because of prevailing northeasterly monsoon. Additionally, it is worth emphasizing that strong tidal currents generate a pair of counter-rotating eddies that significantly dominate the dispersal of the thermal plume. However, seasonal monsoons also play an essential role in modifying the plume's direction and dispersion. The model results reveal that the flow field and thermal plume agree well with observational data.

Keywords: shipboard ADCP; seasonal monsoon; MITgcm; tidal currents; thermal plume

1. Introduction

Nan Wan Bay, situated at the southernmost tip of Taiwan, is a well-known tourist destination and part of the Kenting National Park. The bay is bounded by two capes that extend unequally to the south, as shown in Figure 1. The west cape, locally known as Mou-Bi-Tou (MBT), does not reach as far south as the east cape, locally known as O-Luan-Bi (OLB), does. A seamount exists not far off the southeast point of MBT and partially obstructs the north-south passages. To the south and southwest, Nan Wan Bay opens up to the Luzon Strait (LS) and the South China Sea (SCS), respectively. The semi-enclosed basin is adjacent to the West Pacific Ocean (WPO) to the east and the southern end of the Taiwan Strait to the west. The part of the seamount closest to the surface is at a depth of approximately 50 m [1, 2, 3]. The bay does not have a clear continental shelf on its west side but has a 4km-wide shelf on its east side. Between the seamount to the south and the landmass to the north, the terrain is deep, and this depth extends towards the two capes, forming an open-ended, arc-shaped channel.

Preprints (www.preprints.org) | NOT PEER-REVIEWED | Posted: 3 January 2024 doi:10.20944/preprints202401.0098.v1

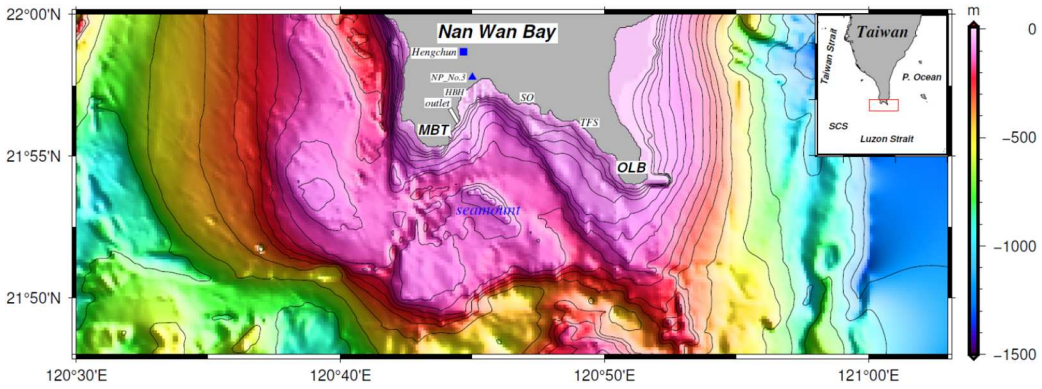

Figure 1. Map, station locations, and topography (in meters) of Nan Wan Bay; the large-scale map at the upper-right corner indicates the study area, model domain, and adjacent seas (generated in the Generic Mapping Tools software package [4]). The triangle denotes the location of the third Nuclear Power Plant in Taiwan, whereas the blue square indicates Hengchun Township.

The movement of water masses in Nan Wan Bay is primarily governed by robust tidal forces including diurnal and semidiurnal tides and is additionally influenced by seasonal monsoons [5, 6]. In the offshore parts of Nan Wan Bay, during ebb tides, the tidal currents typically flow eastward from the southern end of the Taiwan Strait to the western Pacific Ocean through the bay; conversely, they flow westward during flood tides. The tidal range peaks at about 1.6 m during spring tides but decreases to approximately 0.6 m during neap tides. The diurnal and semidiurnal tides have nearly equal energy [1, 2]. Locally, tidal currents are swift, especially outside the bay. During the ebb spring tides, the speed of tidal currents can reach up to 1.7 m/s in and around the bay, especially in the outer of the MBT, where it has been observed to exceed 2 m/s [2]. In the continental shelf on the eastern half of the bay, circulation is relatively straightforward during neap tides, typically following the isobaths, but during flood spring tides, the circulation pattern is more intricate, attributed to the appearance of anticyclonic eddies. On the western side of the bay, cyclonic eddies are easily generated in the flow field during ebb tides, irrespective of whether they are spring or neap tides.

Choi and Wilkin [7] confirmed that thermal plumes, characterized by lighter water density in the regions, generally float on the surface layer to disperse in response to wind forcings [8]. In winter, the northeasterly monsoons usually blow from mid-September to April, peaking in December. Winter monsoons over the local mountain blow down toward the sea surface from the mountaintop. The seaward winds, locally known as downhill winds, become very intense and often lead to the destratification of the water column. The mixing layer's thickness increases from 30 m in summer to 100 m in winter. Summer monsoons are much weaker than winter ones, lasting from July to August [9]. In addition, the sea surface temperature (SST) in Nan Wan Bay is typically 22-26 °C in winter but 24-29 °C in summer [1].

Almost without exception, nuclear power plants are always built near the coast because a large amount of seawater is required to cool down the plant's reactors. Seawater is circulated through a nuclear reactor to transfer or remove heat into seawater, and then the heated seawater forms the thermal waste seawater. This seawater is frequently drained into an area near the shore, such as bays or estuaries, through a long diversion dike [5, 10]. The third Nuclear Power Plant (NP_No. 3) of Taiwan is situated in the inner reaches of Nan Wan Bay, as shown in Figure 1. Through a long diversion dike, considerable thermal seawater (also known as thermal pollution) is discharged into the bay on the east side of the MBT.

Thermal wastewater, whose density is lighter than the source seawater, typically floats on the sea surface layer and flows back and forth due to tidal currents. The fate of the thermal plume dispersal depends on the strength and direction of tidal current, featuring a fortnightly spring–neap cycle As previously mentioned, the presence of eddies, particularly during spring tides, contributes to the complexity of the flow field. In addition to being breeding grounds for countless species of marine life and habitats, coral reefs are very important ecosystems. The coral reefs in Nan Wan Bay

Preprints (www.preprints.org) | NOT PEER-REVIEWED | Posted: 3 January 2024 doi:10.20944/preprints202401.0098.v1

are among the most beautiful marine landscapes in Taiwan; they not only provide a breeding ground for marine animals, forming an ecosystem with considerable biodiversity, but also attract many tourists wishing to appreciate and explore ecosystem. However, the dispersal of the thermal plume from NP_No. 3 conceivably affects the growth and status of the coral reef ecosystem within its vicinity. Therefore, the objective of the present work is narrowly focused on describing the behavior of the thermal plume dispersal from NP_No. 3 during the spring tides in summer and winter.

2. Observations

2.1. Hydrographic data

According to a bulk of historical data, the strong tidal currents dominate the movement of the water mass in Nan Wan Bay. Figure 2 (left panel) shows the selected sea level variations measured in Houbihu Harbor (HBH) from October 1 to 31, 2023, with a pronounced spring–neap cycle. The tidal ranges can reach up to 1.4 m during spring tides but drop to approximately 0.8 m during neap tides. During the spring tides, the flood tide lasts longer than the ebb does because of a similar long-standing wave with a small drop between lower high water and higher high water. Figure 2 (right panel) presents a power spectrum of sea

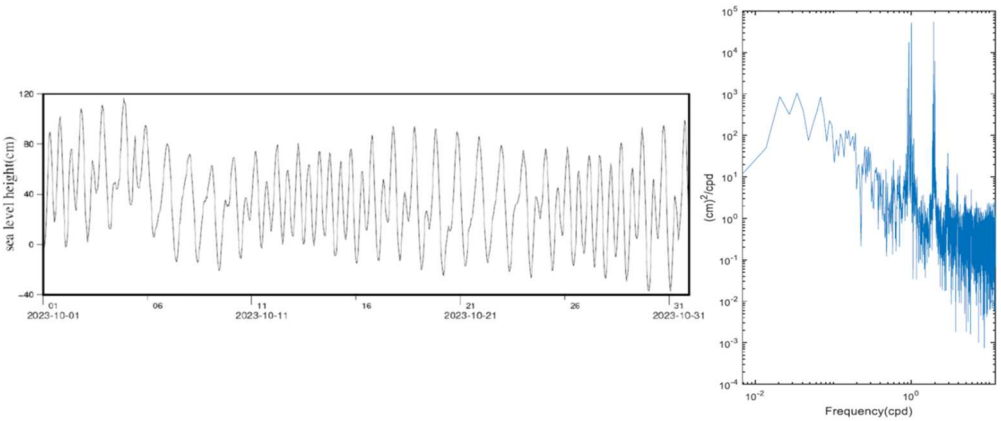

Figure 2. Sea-level time series measured in Houbihu Harbor (HBH) from 1 to October 31, 2023 (left panel), and relative energy spectrum for January 1 to October 31, 2023, with the frequency in the units of cycles per day (right panel).

level height inside a harbor at HBH station; the spectrum contains two peaks corresponding to diurnal and semidiurnal tides, respectively. The relative spectral energies of these peaks are almost equal. As depicted in Figure 2, other frequency spectral energies, except for diurnal and semidiurnal peaks, can be neglected. Figure 3 displays typical temperature and salinity profiles for Nan Wan Bay, obtained from data measured on August 11, 2015 (at 121.8183° E, 21.807° N) and on December 5, 2012 (at 120.6833° E, 21.9662° N), respectively. In summer, the temperature of the surface mixing layer above 50 m reaches 28-29 °C, and beginning from the top of the thermocline layer at approximately 50 m deep, it gradually decreases with increasing depth. In winter, the temperature of the surface mixing layer reaches 25-26 °C and decreases with increasing depth, beginning from approximately 50 m as is the case for summer. As indicated in Figure 3, the salinity profiles for summer and winter are different. In winter, the surface layer salinity is low, significantly approaching a constant value of 33.86 psu throughout the water column with a depth of 0-20 m. However, in summer, the salinity remains at approximately 34.6 psu in the mixing layer, and even in deep water, the salinity also remains different.

Preprints (www.preprints.org) | NOT PEER-REVIEWED | Posted: 3 January 2024 doi:10.20944/preprints202401.0098.v1

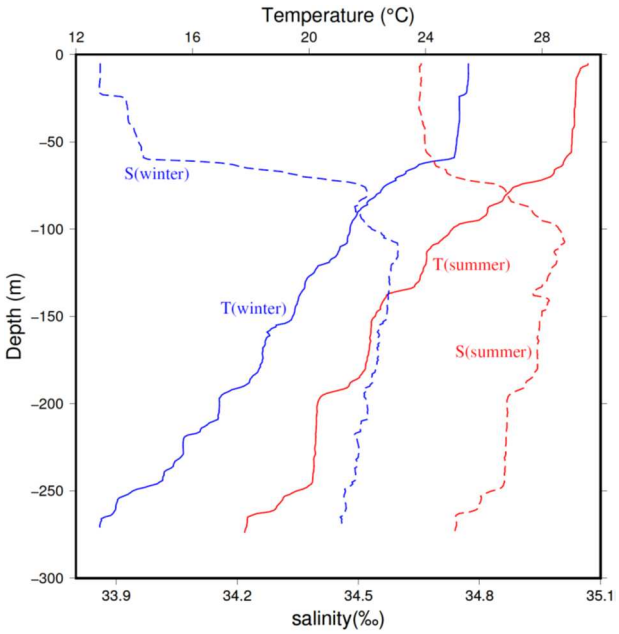

Figure 3. Typical temperature (solid line) and salinity (dashed line) profiles at (120.8183 E, 21.807 N) on August 11, 2015 for summer (red), and at (120.6833 E, 21.9662 N) on December 5, 2012 for winter (blue). .

2.2. Seasonal monsoons

Besides the strong tidal currents that govern water mass motion in Nan Wan Bay, climatological wind stresses are a secondary force influencing circulation. Seasonal monsoons generally modulate the winds in and around Nan Wan Bay. Theoretically, summer monsoons blow gentle southwest winds. Its prevailing period, from July to mid-September, is much shorter than the winter. Subsequently, the winter monsoon prevails in strongly northeast winds until April of the following year, peaking in January [11].

Figure 4 presents stick diagrams of the climatological winds in August and December at the Hengchun weather station of Taiwan's Central Weather Administration (CWA). In Figure 4a, the average wind speed was approximately 3 m/s in magnitude, and the wind blew mainly from the southeast-east direction; however, it sometimes blew with northwest winds for a short period. By contrast, the winds over Nan Wan Bay were expected to blow southwesterly monsoon. A possible cause for this phenomenon is that the mountain surrounding the bay modified the wind's direction because the wind was weak. Conversely, in December 2022 (Figure 4b), strong winds prevailed that originated from the northeasterly monsoon, intensifying the winds to a speed greater than 10 m/s.

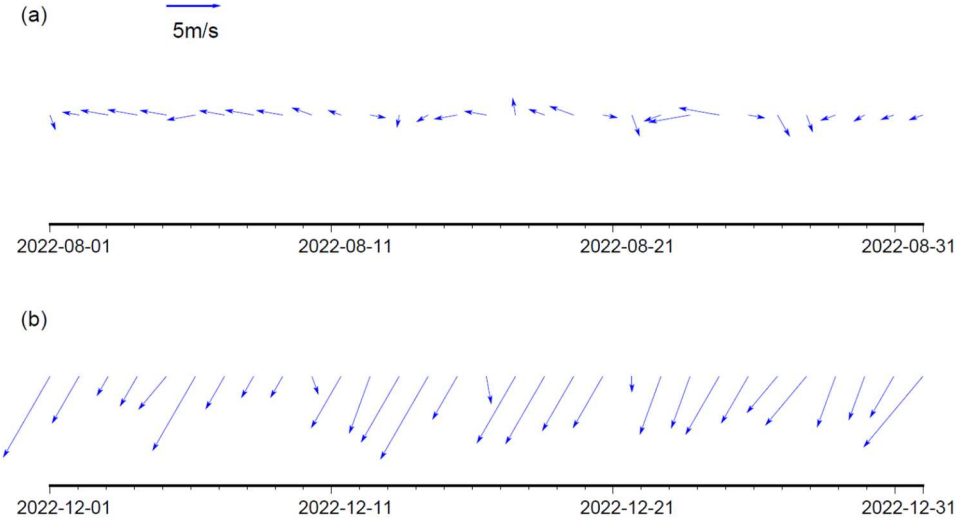

Preprints (www.preprints.org) | NOT PEER-REVIEWED | Posted: 3 January 2024 doi:10.20944/preprints202401.0098.v1

Figure 4. Wind vectors measured at the Hengchun station of the Central Weather Administration (CWA), represented through stick diagrams in (a) summer in August 2022 and (B) winter in December 2022.

2.3. Overall flow fields

In order to understand the comprehensive flow patterns in and around Nan Wan Bay, this study analyzed data collected by an ocean research vessel in fixed-site observations and following a surveying route. Figure 5 illustrates path of the survey conducted by R/V Ocean Researcher III on August 9-11, 2004; the current study conducted a reanalysis of historical shipboard ADCP (Acoustic Doppler Current Profiler) data at a fixed site (labeled F in Figure 5a) and along repeated survey trajectories (Figure 5b). The small setting of the two panels indicates the corresponding observed phase of the local tides. The stick diagram obtained for site F manifested in Figure 6 and indicates the velocity and directions of a fixed point in a flood–ebb tidal cycle for the period of 21:00 on August 10 to 21:14 on August 11, 2004. The sea level variation from the flood tide to the higher high water indicates that the current flowed northwestward at a speed of approximately 0.5 m/s over the aforementioned period. After the peak following the ebb tide, the ebb tidal current flowed southeastward and increased the currents to a speed greater than 1 m/s. It roughly maintained a similar direction to the southeast until the lower high water was approached, at which time the current slowed. Then, after 14:00 August 11, 2004, the tidal current changed its direction back to

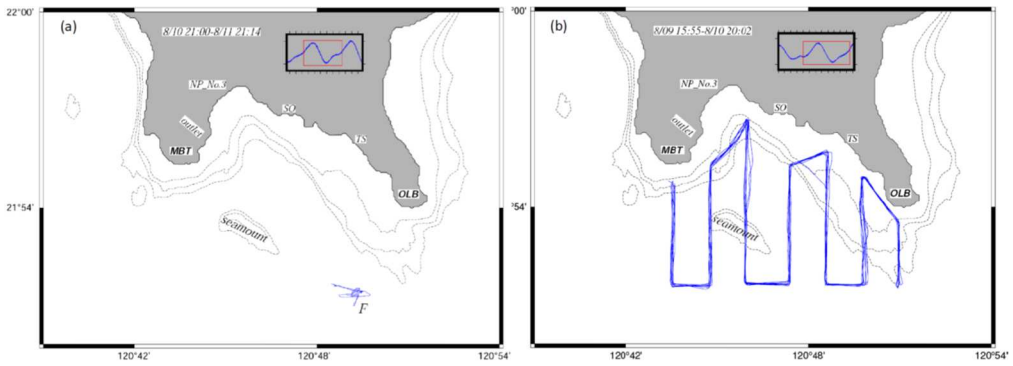

Figure 5. Repeated tracks of shipboard ADCP survey; (a) at fixed site as indicated at F (b) R/V Ocean Researcher III surveying tracks.

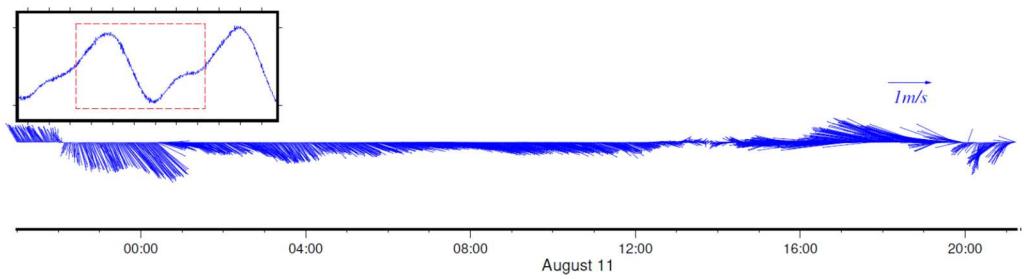

Figure 6. Stick diagram illustrating the current vectors over approximately 24 hours; a small setting inserted in the upper left corner indicates the sea level fluctuations.

approximately northwest or southwest. In order to ensure as many of the synoptic features as possible are retained, tidal current patterns obtained from 8 track of the trajectory are presented; each track was obtained in approximately 3.3-3.7 hours between 15:55 on August 9 to 20:02 August 10, 2004, as shown in Figure 5b. Figure 7 presents the tidal flow fields at a depth of 10.4 m in the 8 tracks. The red rectangle in a small setting for each panel in Figure 7 indicates the period of the tidal phase during which the track was performed. Figures 7a, 7b, and 7c show the tidal flow pattern from lower

Preprints (www.preprints.org) | NOT PEER-REVIEWED | Posted: 3 January 2024 doi:10.20944/preprints202401.0098.v1

high water to higher high water. As indicated in Figure 7a, currents off the outer of MBT flowed west-southwestward, whereas currents off the south of OLB moved eastward; the currents in and around the bay were sluggish, with an average speed of less than 0.05 m/s. The patterns in Figures 7b and 7c resemble that in Figure 7a but with a notable difference in the strength of the flow; the flows presented in Figures 7b and 7c are much weaker than that in Figure 7a. Over the slack water of the higher high water, the ebb tidal currents launched and began to flow eastward, with the currents being particularly prevalent off MBT in Figure 7d.

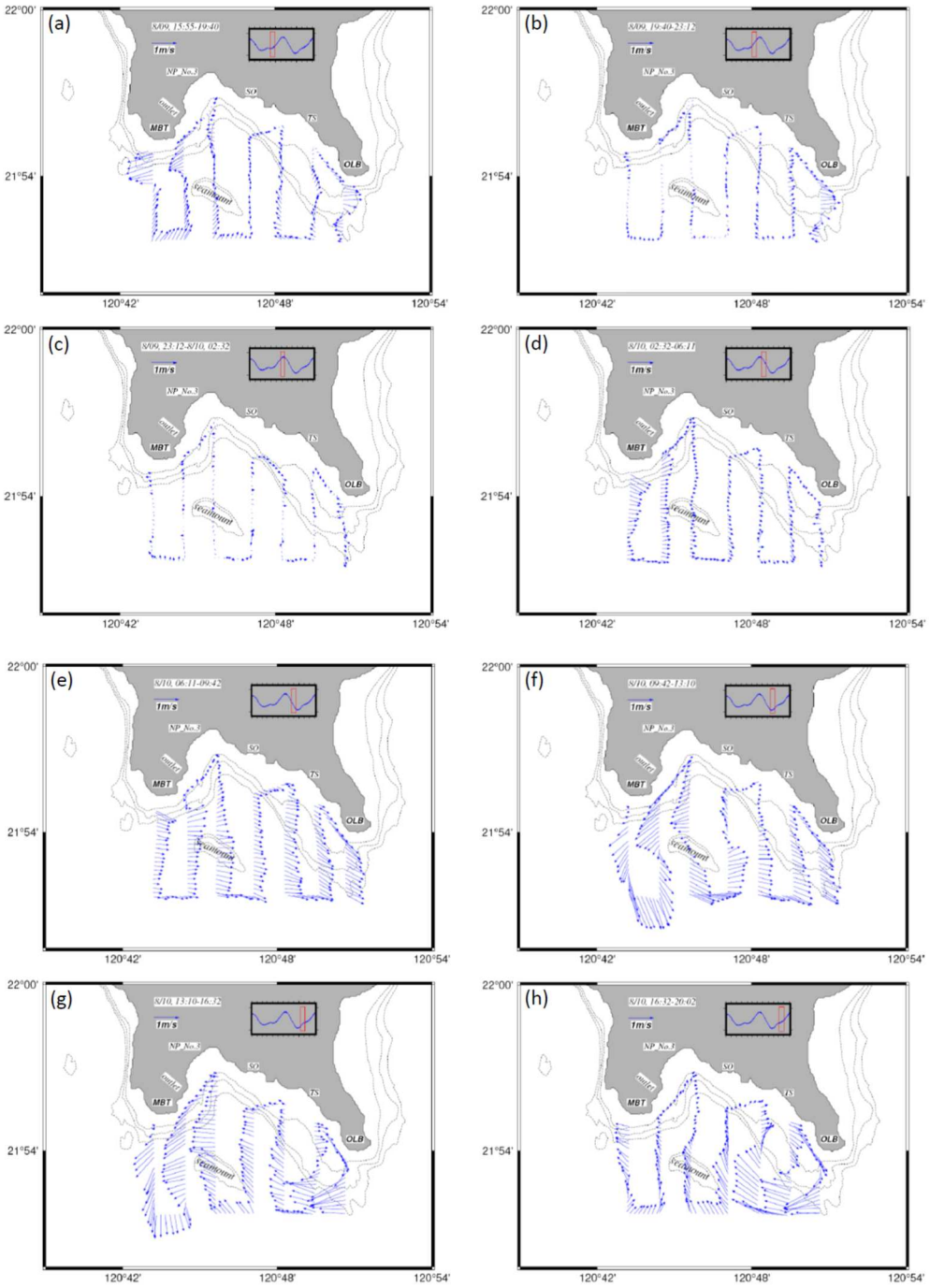

Figure 7. Surface currents at 8-m depth derived from the Ocean Researcher III survey during (a) 15:55-19:40 on August 9, (b) 19:40-23:12 on August 9, (c) 23:12 on August 9-02:32 on August 10, (d) 02:32-06:11 on August 10, (e) 06:11-09:42 on August 10, (f) 09:42-13:10 on August 10, (g) 13:10-16:32 on August 10, (h) 16:32-20:02 on August 10. Insets: red rectangles indicate the tidal phase period.

Preprints (www.preprints.org) | NOT PEER-REVIEWED | Posted: 3 January 2024 doi:10.20944/preprints202401.0098.v1

Figure 7e manifests the entire ebb flow field in and around the bay and indicates strong easterly currents with a speed greater than 1 m/s. With the exception of those in the most eastward flow pattern, the currents in the inner reaches around MBT exhibited a tendency toward cyclonic eddy in the phase period. As indicated in Figure 7f, the flow pattern outside the bay indicates typical flows similar to those presented in Figure 7e, but also a sizeable cyclonic eddy circulates the seamount to flow. Meanwhile, the flows were quite strong, irrespective of whether they were a typical ebb flow or circulating cyclonic eddy. Over the slack water of the lower low water, the flow pattern rapidly changed direction from eastward to westward and reached a high velocity, and an anticyclonic eddy formed to the southwest of OLB, as shown in Figure 7g. Figure 7h shows that an energetic anticyclonic eddy circulated over the continental shelf and the deeper reaches on the southwest side of OLB. During this phase, a well-defined anticyclonic eddy emerged in the region exhibited a robust circulating speed even in excess of 1.32 m/s.

2.4. satellite images

A comprehensive approach was employed to assess the range of impact of the thermal wastewater discharged from the Third Nuclear Power Plant on the nearby ecosystem. Landsat 8 satellite images for 2018-2022 were used to analyze the patterns of plume dispersion. The Landsat 8 satellite payload contains the Operational Land Imager (OLI) and Thermal Infrared Sensor (TIRS). The size of the scenes captures by Landsat 8 is 185 km x 180 km, and the images employed in this study were acquired at approximately 10 AM local time. The spatial resolutions are 30 m and 100 m for the visible and thermal bands, respectively. Hence, Landsat 8 has sufficient scene coverage and spatial resolution to enable an investigation of the thermal plume discharge of the third Nuclear Power Plant. Figure 8 displays the SST fields around the western side of Nan Wan Bay, with snapshots selected at specific instances. Figure 8a indicates that the thermal plume from the outlet of the NP_No.3

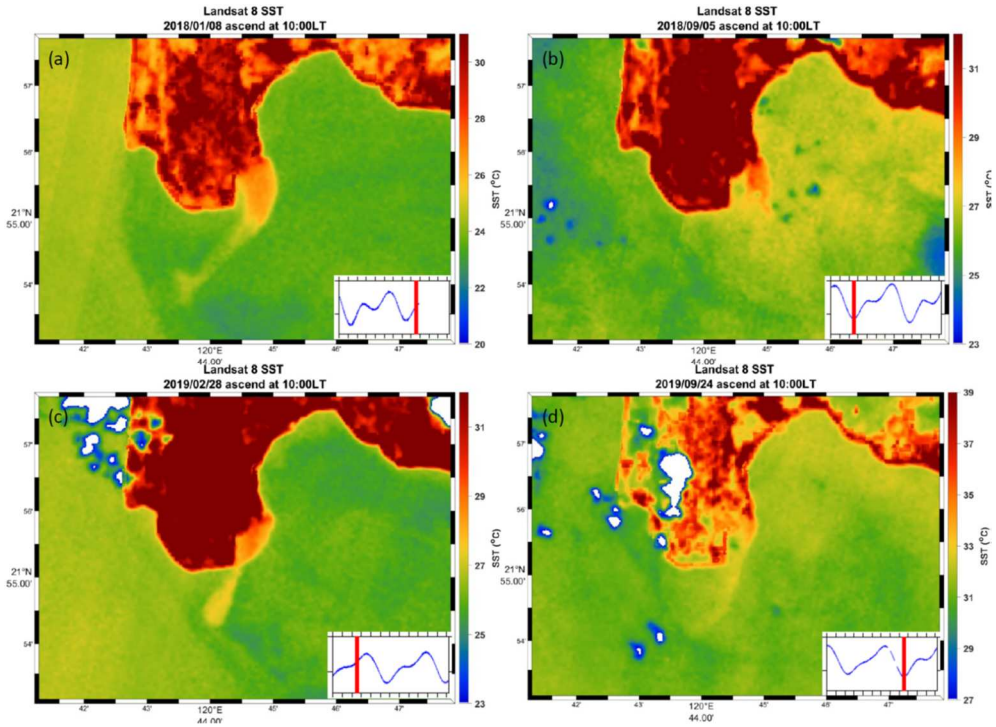

Preprints (www.preprints.org) | NOT PEER-REVIEWED | Posted: 3 January 2024 doi:10.20944/preprints202401.0098.v1

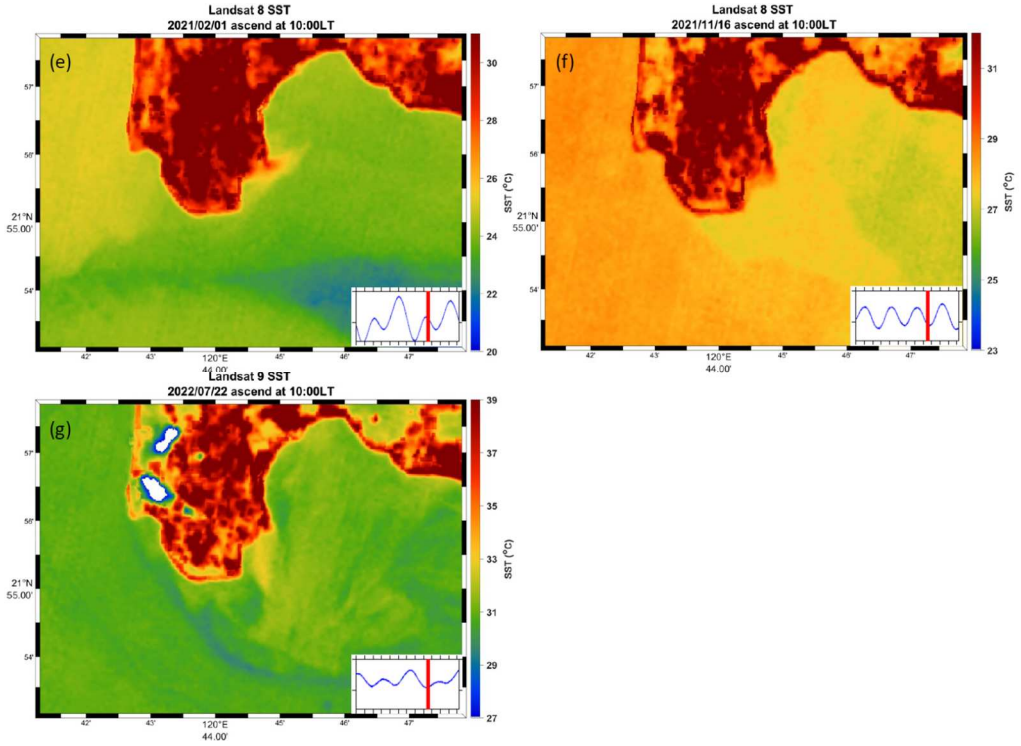

Figure 8. Satellite images showing the instantaneous SST derived from Landsat 8 at (a) 10:00 on August 1, 2018; (b) 10:00 on September 5, 2018; (c) 10:00 on February 28, 2019; (d) 10:00 on September 24, 2019; (e) 10:00 on February 1, 2021; (f) 10:00 on November 16, 2021; (g) 10:00 on July 22, 2022. A small setting with vertical red line in the lower right corner indicates the local tidal phase.

does not flow directly to the southeast, which is the direction of the diversion-dike. Instead, the thermal plume follows the eastern side of MBT and flows along the western coast of the bay to the south while approaching the lower high water. A part filament of the thermal plume leaves the MBT coast and enters the nearshore sea area. During the phase of the lower low water, the NP_No.3 thermal plume directly streams to the south, and the thermal plume front seems to be rapidly advected and diluted (Figure 8b), indicating the plume disperses within a small area before disappearing. Over the higher low-water slack, as shown in Figure 8c, the plume exhibits behavior similar to that depicted in Figure 8a. However, it seems to more closely adhere to the MBT coast and leaves the cape toward the south-southwest. While the phase stays at the slack of the lower low water, as illustrated in the small setting in Figure 8d, the thermal plume swifts to the south and becomes a narrow band filament that is advected to the offshore region. Accordingly, while the phase between higher high water and lower low water, the flow field in the bay prevails the ebb tidal currents, peaking at the phase of lower low water and easily generating cyclonic eddy. In Figure 8e, the thermal plume immediately turns to the northeast when it leaves the outlet. As a result, the thermal plume's behavior is affected by advection of an anticyclonic eddy, leading to the plume flowing northeastward. In Figure 8f, the thermal plume seemingly disappears from the image; strictly to be said, it has accumulated in the left corner of the diversion dike during the neap ebb tide. During the lower low water phase (Figure 8g), as the modulated spring–neap tidal cycle proceeds into the early spring tide stage, the thermal plume, carried by the cyclonic eddy, flows southward. This situation is similar to that presented in Figure 8d, although the plume filament moves as far southward as it does in Figure 8d.

3. Model description and setups

3.1. Model description

MITgcm is a time-marching, circulating ocean model with nonhydrostatic capabilities and is suitable for studying a wide range of phenomena[12, 13, 14]. MITgcm, a three-dimensional circulation

Preprints (www.preprints.org) | NOT PEER-REVIEWED | Posted: 3 January 2024 doi:10.20944/preprints202401.0098.v1

model, is utilized to examine and predict the dispersal of the thermal plume from the third Nuclear Power Plant in Nan Wan Bay. More details for the model information are described in its documentation (https://mitgcm.readthedocs.io/en/).Under Boussinesq and hydrostatic approximation, the model solves equations for three-dimensional momentum, temperature, salinity, and continuity. The study domain of the present work ranges from 120.5° to 121.05° in longitude and from 21.8° to 22° in latitude (Figure 1), with a horizontal resolution of 200 m, meaning that the horizontal grid size (i.e., dx or dy) equals 200 m. In the vertical direction resolution, 35 layers are adopted in the model, and each layer's thickness corresponds to that in the U.S. Navy's Global Hybrid Coordinate Model (HYCOM; More details regarding the model information are given at https://www.hycom.org/). As shown in Figure 1, the topographic data of the present research domain are obtained from the Ocean Data Bank (ODB) of the Nation Science and Technology Council (NSTC) of Taiwan and privately collected through a fishing boat.

3.2. Boundary and initial conditions

During the flood-tide period, a tidal wave propagates from the West Pacific Ocean to Taiwan Island, and after impacting the landmass, it separates into two flood-tidal waves. The southward wave runs along the southeastern coast of Taiwan, rounds the OLB into Nan Wan Bay, and passes the MBT, heading toward the Taiwan Strait. Conversely, the ebb tidal wave propagates from the Taiwan Strait into Nan Wan Bay and flows northward into the West Pacific Ocean during the prevailing ebb tides. Hence, for the model open boundaries, tidal currents can flow in and out freely at only the northern boundary. During the flood tides, the tidal currents flow perpendicular to the northeastern open boundary into the model domain and flow perpendicularly out of the model domain from the northwestern open boundary. Parallel to the northern open boundary, the tangential component velocities are specific to be zero. The remaining open boundary conditions—including those for the eastern, southern, and western boundaries, are described as follows [8].

$$\frac{\partial}{\partial n}(u, v, T, S) = 0 \tag{1}$$

where n is normal to arbitrary open boundaries; parallel to these boundaries, their tangential velocities are set as indicated below.

$$\frac{\partial}{\partial y}(u, T, S) = 0 \tag{2}$$

$$\frac{\partial}{\partial x}(v, T, S) = 0 \tag{3}$$

The observed characteristic temperature and salinity profiles displayed in Figure 3 are adopted for all open boundaries and initial conditions. For the sea surface, no momentum, heat, or salt flux is input, but winds in summer and winter are imposed. Regarding the variable bottom boundary as follows.

$$\frac{\partial}{\partial z}(T, S) = 0 \tag{4}$$

$$\upsilon \frac{\partial}{\partial z}(u, v) = b(u^2 + v^2)^{1/2}(u, v) \tag{5}$$

where b is a dimensionless bottom drag coefficient with 0.0025 in magnitude. Details regarding the model formulation are provided in Lee et al. [14].

3.3. Tidal driving force

The initial model is of a motionless ocean; tidal currents are then imposed on the northeastern and northwestern boundaries. The oscillating tidal currents are transformed from diurnal and semidiurnal tidal constituents (M2, S2, N2, K2, K1, O1, P1, and Q1) obtained from the NAO.99b data

Preprints (www.preprints.org) | NOT PEER-REVIEWED | Posted: 3 January 2024 doi:10.20944/preprints202401.0098.v1

bank [15]. The transformation from sea level variation into oscillating tidal currents is described in more detail in [16]. Except for driving forces of the northeastern and northwestern boundaries, summer and winter monsoons (Figure 4) are also imposed on the model sea surface in the different seasons. In order to study the NP_No.3 thermal plume, the water flux through the diversion dike is specified as being 121.3 m^3/s in summer and 61.2 m^3/s in winter (https://cwms.ptepb.gov.tw/PUBLIC/RealTime/Get_AVGR.aspx). In addition to the water flux, the discharge temperature in the dike is set to 36.4 °C and 34.2 °C for summer and winter, respectively. The released position of the thermal plume is located at the upstream boundary, approximately 5 grid spaces from the mouth of the diversion dike. To ensure that the temperature and salinity fields remain stable, restoration forcings are adopted for nudging these fields toward initial hydrographic fields. The restoration rate for temperature and salinity fields is set to 30 days (i.e., using the RBCS package). The mixing coefficient is 8 m^2/s for momentum equation and 0.8 m^2/s for temperature and salinity equations in the horizontal directions. Irrespective of whether dynamic momentum or thermohaline is being considered, the nonlocal K-Profile Parameterization scheme (KPP) is adopted to account for various unresolved mixing in the vertical direction [17]. Starting from an initially motionless state, the model runs for a month with a time step of 18 seconds. The results from the final 10 days are sampled instantaneously for the discussion below, specifically during the spring tides.

4. Numerical model results

4.1. Circulation and upwelling regions

Although the model executed the fortnightly spring–neap cycles, the day-to-day flow field changes were highly visible. Quasicyclical stationary equilibrium on a daily time scale can be rapidly reached at approximately 2 days if the model is computationally stable. The results from the final 10 days in the simulation were sampled instantaneously for the discussion, with a focus on the results for the spring periods.

Figure 9 illustrates the model-produced surface circulation and surface temperature fields for summer and winter. In winter, the prevailing ebb tidal currents from off the northwestern coast of the Hengchun peninsula pass by MBT, and partial currents enter the bay to form a cyclonic eddy during the phase between the lower low-water and lower high-water stages (Figure 9a). These ebb currents to the east

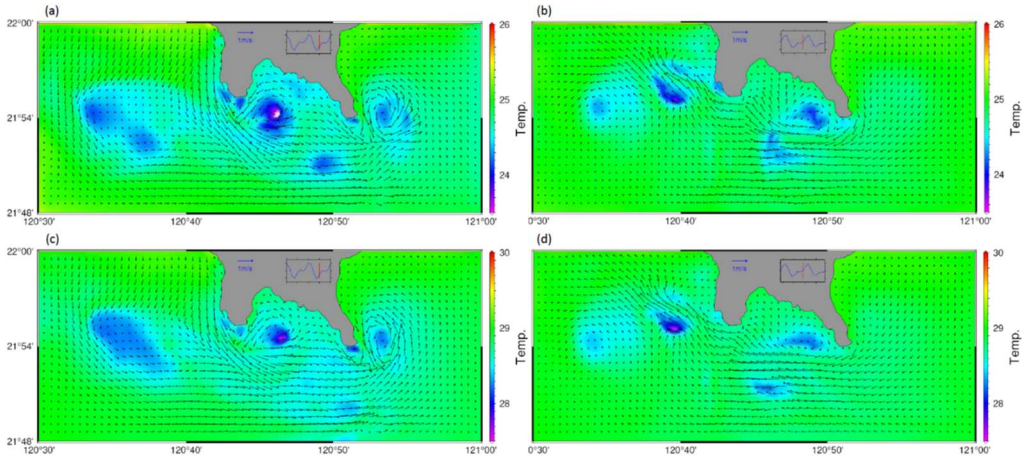

Figure 9. Model-produced tidal currents and temperature fields in the surface layer during (a) the ebb tide in winter; (b) the flood tide in winter; (c) the ebb tide in summer; (d) the flood tide in summer. Sea level marked by a vertical red line indicates the tidal phase inserted at a small setting in the upper right corner in each panel.

of the eddy center flow northward onto the shelf, impact the shallow coast, and then separate two ways. One set of currents flows northwestward to complete the eddy circulation; the other flows southeastward along the continental shelf, leaving Nan Wan Bay from OLB and then entering the

Preprints (www.preprints.org) | NOT PEER-REVIEWED | Posted: 3 January 2024 doi:10.20944/preprints202401.0098.v1

Pacific Ocean. It is worth noting, i.e., the ebb tidal flow passing OLB also forms a robust cyclonic eddy to the east of OLB.

The ebb-tide cyclonic eddy in the western part of the bay induces local upwelling of cold water around the eddy center. This temperature characteristic agrees with the historical data, as shown in Figure 9a. Visibly, the cold water upwelling on the western side of the bay is more robust than that on the east side of OLB. During the flood tides in winter (Figure 9b), a westward flood tidal current from the northeastern offshore region of the Hengchun peninsula that flows over the shallow bottom to south of OLB gains anticyclonic vorticity and then deflects into Nan Wan Bay. Some of the currents flow northward onto the continental shelf to form an anticyclonic eddy to the west of OLB during the phase over the lower high water. Cold water upwelling is found around the anticyclonic eddy's center but much weaker than that occurring with prevailing ebb tidal currents. Similar to in winter, in summer, southeastward ebb currents flow into the bay, and some of the currents flow northward to form a cyclonic eddy during the phase of the lower low water. Although the sea level is in the same phase as that in winter, the outlines of cyclonic eddies are slightly different, as is strength, because of seasonal monsoon effects. The model-produced temperature drops around the centers of the cyclonic eddies decreases to a smaller degree than it does in winter, as illustrated in Figure 9c. Figure 9d presents a snapshot of the model-produced flow and temperature fields in summer during the period of the higher low water. Because of the influence of different monsoon effects, the feature shapes of the model-produced anticyclonic eddy in Figure 9d are distinguishable in winter and summer. Meanwhile, the anticyclonic-induced low-temperature anomaly in the eddy center is dispersed chiefly to the west, and the area over which it diffuses is smaller than it is in winter.

Many flow fields and temperature patterns in Nan Wan Bay are mentioned in the preceding paragraphs, irrespective of whether they are observed data or numerical model results. The flood-ebb tidal currents generate a pair of counter-rotating eddies that modify how the thermal plume disperses off the outlet mouth. In order to quantify model output, the model temperature, defined as exceeding 29 °C in summer (25 °C in winter), is used to indicate the NP_No.3 thermal plume source.

4.2. Thermal plume dispersal in summer

Figure 10 illustrates the model-produced thermal plume in summer around the inner reaches of MBT in a diurnal cycle during the spring tide. The tidal phase concerning the diurnal cycle is inserted with a small setting in the left corner of each panel. In Figure 10a, the thermal plume during the lower low-water phase, with the temperature exceeding 29 °C, disperses southwestward along the coast. At this time, the prevailing ebb tidal current generates a relatively minor cyclonic eddy off the southeastern coast of MBT. The returning flow of the eddy circulation close to the coast of MBT pushes the thermal plume from the

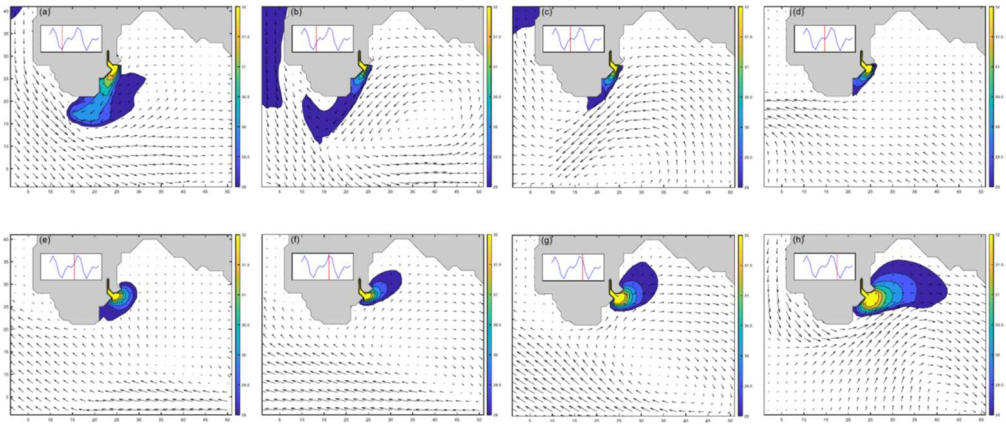

Figure 10. Model-produced tidal currents and thermal plume fields at the surface in summer. Panels (a, b, c, d, e, f, g, and h) are related to tidal phases, respectively. A small inset in the upper left corner, featuring the sea level marked by a vertical red line, indicates the model tidal phase.

Preprints (www.preprints.org) | NOT PEER-REVIEWED | Posted: 3 January 2024 doi:10.20944/preprints202401.0098.v1

outlet's mouth to the southwest. The thermal plume front touching the prevailing ebb currents south of MBT is quickly advected and dissipated. Therefore, such a flow field restricts the thermal plume dispersal to the northeast and the inner reaches of the bay. When the sea level phase is between the lower low water and lower high water, as depicted in Figure 10b, a fully developed cyclone almost completely occupies the western part of the bay, accompanied by a swift tidal current to the south of MBT that flows southeastward. At this time, the thermal plume carried by the shear flow of the eddy's periphery becomes a narrow-and thermal filament streaming toward the southwest. A recirculating current in the shadow zone, south of MBT, even carries some of thermal plume to the northwest. Because the sea level phase is transitional at the lower high water (Figure 10c), the fully developed cyclone gradually weakens and then converts to flood tides. However, the southwestward shear flow of the eddy outer ring remains intense. Visibly, the thermal plume adheres to the coast of MBT, and the previous thermal plume, flowing northwestward from south of MBT, also retracts to form a narrow band. Figure 10d shows that a weak flood current from the southeast directly flows northwestward to MBT during the phase between lower high water and higher low water. The thermal plume is confined to the north of MBT, and the high-temperature (exceeding 32 °C) thermal plume is accumulated near the outlet due to the weak flow field. Similar to the situation shown in Figure 10e, the thermal plume disperses forward due to a large amount of high-temperature water accumulating at the outlet. As depicted in Figure 10f, the thermal plume accumulated in the outlet front begins moving to the northeast, driven by the northeastward shear flow of the anticyclonic eddy's periphery. A fully developed anticyclone covers Nan Wan Bay, and the intense shear flow pushes more high-temperature water to the northeast during the phase over the higher high water, as illustrated in Figure 10g. Subsequently, the anticyclonic shear flow is enhanced by ebb tidal currents from the northwest of the Hengchun peninsula, giving rise to more high-temperature water being pushed toward the inner reaches of the bay during the phase between higher high water and lower low water, as shown in Figure 10h.

4.3. Thermal plume dispersal in winter

Actually, the winter thermal plume is similar to that in summer at the same phase in relation to the same diurnal cycle during the spring tides.

If any, the thermal plume dispersal would be attributed to the influence of distinct seasonal monsoons. In Figure 11a, a minor cyclonic eddy develops initially near the southeastern side of MBT and, concurrently, a southeastward tidal current develops to the south. The returning flow of the eddy circulation close to the coast of MBT drives the thermal plume from the diversion dike's mouth to the southwest. At this time, the thermal plume disperses along the MBT coast toward the southeast, and the front of the plume touches the prevailing ebb currents south of MBT, at which time the plume is quickly advected and diluted. As shown in Figure 11b, as the sea level phase falls between lower low water and lower high water, a fully developed cyclone covers the bay's western side,

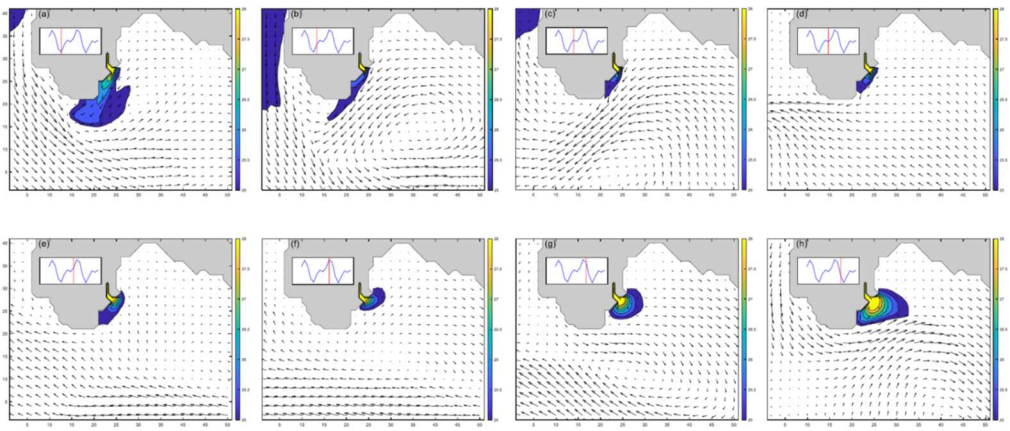

 doi:10.20944/preprints202401.0098.v1

Figure 11. Model-produced tidal currents and thermal plume fields at the surface in winter. Panels (a, b, c, d, e, f, g, and h) are related to tidal phases, respectively. A small inset in the upper left corner, featuring the sea level marked by a vertical red line, indicates the model tidal phase.

with the cyclone accompanied by a swift tidal current to the south of MBT and flowing southeastward. At this time, the thermal plume becomes a narrow-band thermal filament streaming toward the southwest because the plume is compressed by the shear flow of the eddy periphery. While the sea level phase is transiting at the lower high water in Figure 11c, the fully developed cyclone weakens and is gradually converted to a flood pattern, but the southwestward shear flow of the eddy outer ring remains intense. Visibly, the thermal plume forms a small, narrow band adhering to the MBT coast. Figure 11d is also similar to the situation in Figure 11c when the tidal phase is at higher low water, and the flood tidal current begins to launch. The thermal plume appears confined to the north of MBT, of which the high-temperature water (exceeding 28 °C) becoming concentrated in the outlet. This is similar to the results shown in Figure 11e, during the sea-level phase between higher low water and higher high water, the thermal plume dispersion is confined to the zone surrounding the outlet because the northwestward flow fields is weak. As illustrated in Figure 11f, the thermal plume, which slightly accumulated in the outlet front, begins drifting to the northeast, being driven by the northeastward shear flow of the anticyclonic eddy. Subsequently, a well-developed anticyclone covers Nan Wan Bay, and the shear flow pushes the thermal water to the southeast during the phase over the higher high water, as shown in Figure 11g. The situation in which the plume disperses southeastward from the outlet differs from that presented in Figure 10g, in which the considerable thermal plume drifts to the northeast. As shown in Figure 11h, the anticyclonic shear flow subsequently combines with the ebb tidal currents coming from the western side of MBT, leading to more high-temperature water being pushed toward the east during the phase between the higher high water and lower low water. Simultaneously, much of the high-temperature water (greater than 28 °C) seemingly accumulates around the outlet front.

5. Discussion and conclusions

In this study, we incorporated tides and daily wind forcings into the MITgcm model to examine their effects on the thermal plume of NP_No.3 and the circulation in Nan Wan Bay. Regardless of flow fields or thermal plumes, the model results agreed favorably with observational data, which comprise satellite images and shipboard ADCP surveys. In light of the output results, the model captured the major circulation features, which revealed that the current from the west side of MBT flows around MBT into the bay during early ebb tides (figure not shown). The weak ebb current often flows southeastward along the isobaths, running more or less parallel to the coastline, as shown in Figures 7d and 7e. As the sea level progresses to the lower low-water phase, a well-developed cyclonic eddy covers the western part of Nan Wan Bay, accompanied by a fast and southeastward-flowing tidal current to the south of MBT. Our model results and the findings of the shipboard ADCP survey both captured the corresponding flow patterns (Figures 7f and 9a). The thermal plumes (Figures 10a and 10b) derived from the model results corresponded to those of the Landsat 8 SST in summer, as indicated in Figures 8b, 8d, and 8g. The recirculating flow of a cyclonic eddy, adhering to the inner MBT coast, pushes the thermal plume to stably flow southwestward. We propose that the force pushing the thermal plume southwestward always exists when the sea level is between the higher high water and the mid-lower high water, i.e., that a cyclonic eddy dominates the ocean circulation on the west side of the bay.

Interestingly, a well-developed anticyclone subsequently covers Nan Wan Bay during the tidal phase between the higher low water and higher high water, as shown in Figures 9b and 7h, and the currents of the anticyclonic outer ring in the south flow northwestward to impact the thermal water pool at the outlet's mouth. As a result, this leads to some of the thermal plume being pushed to the northeast by the north-separated branch, as shown in Figures 8e, 10e, and 10f. In summer, as the anticyclonic eddy gradually expands, the direction in which the thermal plume disperses appears to become more consistent with the eddy outer-ring circulation indicated in Figures 10f and 10g. In

Preprints (www.preprints.org) | NOT PEER-REVIEWED | Posted: 3 January 2024 doi:10.20944/preprints202401.0098.v1

winter, the strong northeasterly monsoon acts as an opposing force on the sea surface, resulting in the anticyclonic eddy structure being destroyed, as shown in Figure 9d. As is the case with the prevailing northeasterly monsoon, the northeastward thermal plume is suppressed and further turns to disperse eastward, as indicated in Figures 11f, 11g, and 11h. In summer, the thermal plume in the same phase

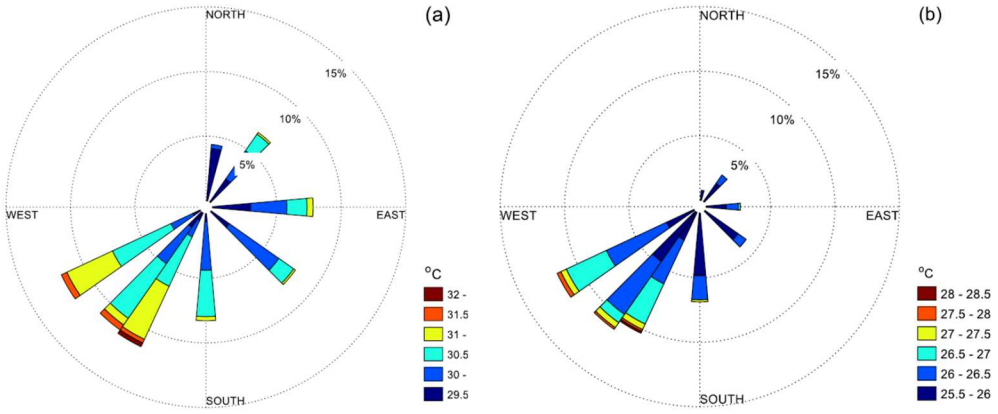

Figure 12. Rose diagrams indicating the direction of thermal-plume dispersal and thermal accumulation in (a) summer and (b) winter.

appears to diffuse to the northeast during the prevailing mild southwesterly monsoon, as displayed in Figures 10f, 10g, and 10h. Model stations around the outlet at a distance of approximately 500 m were sampled to create the rose diagrams, as displayed in Figure 12.

As indicated in Figure 12a, the thermal plume is highly likely to disperse to the southwest (43%) in summer, although there is also a low probability of it drifting to the southeast (15%) or northeast (10.5%) because of the influence of the gentle southwesterly monsoon. In winter, as shown in Figure 12b, the thermal plume is most likely to disperse to the southwest (40.5%) and highly unlikely to disperse to the northeast (3.5%) or southeast (5.5%) due to influence of the prevailing northeasterly monsoon.

In conclusion, it is worth emphasizing that strong tidal currents generate a pair of counter-rotating eddies that significantly dominate the dispersal of the thermal plume, but seasonal monsoons also play an essential role in modifying the plume's direction and dispersion.

Author Contributions: Conceptualization, H.J.L., S.J.H., P.J.M. and C.C.C.; methodology, H.J.L. ,Y.C.T. and C.Y.H.; software, C.Y.H. and Y.C.T.; validation, H.J.L.; formal analysis, S.J.H, Y.C.T. and C.Y.H.; investigation, P.J.M. and C.C.C.; writing—review and editing, H.J.L. All authors have read and agreed to the published version of the manuscript.

Data Availability Statement: The topographic and hydrological observed data that support the findings of this study are openly available in the ODB of the National Science and Technology Council (NSTC), Taiwan, at https://www.odb.ntu.edu.tw/en/. The ADCP that support the findings of this study are available on request from the NSTC, Taiwan, at https:// www.odb.ntu.edu.tw/en/. These datasets (satellite images) are derived from the following public resources at https://www.usgs.gov/landsat-missions/landsat-8. These datasets (seal level heights and winds) supporting the findings of this study are available on request from the Central Weather Administration (CWA), Taiwan, at https://e-service.cwa.gov.tw/wdps/.

Acknowledgments: Authors H.-J. Lee, C.-Y. Ho, and Y.-C. Tsai were supported by the NSTC of Taiwan under grant NSTC 112-2611-M-019-016. Author S.-J. Huang was supported by the CWB of Taiwan under grant CWB 112H80506, CWB 111H80506 and MOST 108-2611-M-019-018. Author P.-J. Meng was supported by the MOST and NSTC of Taiwan under various grants MOST 111-2611-M-259-002, MOST 110-2611-M-259-002, MOST 109-2611-M-259-003, MOST 108-2611-M-291-005, MOST 107-2611-M-291-001, and MOST 106-2611-M-291-006.

Conflicts of Interest: The authors declare no conflict of interest.

References

1. Lee, H.J., Chao, S.Y., Fan, K.L., Wang, Y.H., Liang, N.K. Tidally induced upwelling in a semi-enclosed basin: Nan Wan Bay. *J. Oceanogr.* 1997, *53*, *467–480.* **[CrossRef]**
2. Lee, H.J., Chao, S.Y., Fan, K.L. Flood-ebb disparity of tidally induced recirculating eddies in a semi-enclosed basin: Nan WanBay. *Cont.l Shelf Res.* **1999a**, *19(7), 871–890.* [CrossRef]
3. Lee, H.J., Chao, S.Y., Fan, K.L., Kuo, T.Y. Tide-induced eddies and upwelling in a semi-enclosed basin: Nan Wan. *Estuarine, Coastal Shelf Sci.* ***1999b***, 49(6), 775–787. [CrossRef]
4. Wessel, P., Luis, J.F., Uieda, L., Scharroo, R., Wobbe, F., Smith, W.H.F., Tian, D. The Generic Mapping Tools version, *Geochem. Geophy. Geosy*. **2019**, 20, 5556–5564. [CrossRef]
5. Chen, C.T.; Jan, S.; Chen, M.-H.; Liu, L.-L.; Huang, J.-F.; Yang, Y.-J. Far-Field Influences Shadow the Effects of a Nuclear Power Plant's Discharges in a Semi-Enclosed Bay. *Sustainability*. **2023**, *15*, 9092. [CrossRef]
6. Jan S., Chen C.T., Tu Y.Y., Tsai H.S. Physical properties of thermal plumes from a nuclear power plant in the southernmost Taiwan. *J Mar Sci Technol*. **2004**, 12:433–441. doi: 10.51400/2709-6998.2265. [CrossRef]
7. Choi, B.J., Wilkin, J.L. The effect of wind on the dispersal of the Hudson River plume. *J. phys. Oceanogr.* ***2007***, *37*(7), 1878-1897. [CrossRef]
8. Chao, S.Y. Tidal Modulation of Estuarine Plumes. *J. Phys. Oceanogr.* ***1990***, **20**, 1115–1123, [CrossRef]
9. Lee, H.J., Chao, S.Y. A climatological description of circulation in and around the East China Sea, *Deep Sea Res. Part II.* ***2003***, Vol 50, 6–7, 1065-1084, [CrossRef]
10. Laguna-Zarate, L., Barrios-Piña, H., Ramírez-León, H., García-Díaz, R., Becerril-Piña, R. Analysis of Thermal Plume Dispersion into the Sea by Remote Sensing and Numerical Modeling. *J. Mar. Sci. Eng.* **2021**, *9*(12), 1437. [CrossRef]
11. Lee, H.J., Liu, K.K. Tidal effects on Changjiang plume dispersal in the East China Sea. *J. Mar. Sci. Tech.* **2013**, Vol. 21: Iss. 3, Article 13. DOI: 10.6119/JMST-013-0207-1 [CrossRef]
12. Marshall**,** J., Jones, H., Hill, C.N. Efficient ocean modeling using non-hydrostatic algorithms. *J. Marine Syst.* ***1998***, **18**, 115-134, [CrossRef]
13. Marshall, J., Shuckburgh, E., Jones, H., Hill, C. Estimates and implications of surface eddy diffusivity in the southern ocean derived from tracer transport. *J. Phys. Oceanogr.* ***2006***, **36**,1806–1821, [CrossRef]
14. Lee, H.J., Lee, M.A., Ho, C.Y., Hsu, P.C., Wang, Y.C. Crescent-Shaped Low-Temperature Distribution along the Convex Topography in the Southeastern Edge of Taiwan Bank in Summer. *J. Phys. Oceanogr.* ***2002***, **52**, 2705–2723, [CrossRef]
15. Matsumoto, K., Takanezawa, T., Ooe, M. Ocean tide models developed by assimilating TOPEX/POSEIDON altimeter data into hydrodynamical model: A global model and a regional model around Japan. *J. Oceanogr.* ***2000***, *56*, 567-581. [CrossRef]
16. Ho, C.Y.; Fang, T.H.; Wu, C-H.; Lee, H.J. Interplay between Asian Monsoon and Tides Affects the Plume Dispersal of the New Hu-Wei River off the Coast of Midwest Taiwan. *Water.* **2022**, *14*, 152. [CrossRef]
17. Large, W.G., McWilliams, J.C., Doney, S.C. Oceanic vertical mixing: A review and a model with a nonlocal boundary layer parameterization. *Rev. Geophy.* ***1994***, *32*(4), 363-403. [CrossRef]